Hyperfine Interactions 62(1990)353 – 358

TDPAC CHARACTERIZATION OF TIN OXIDES USING ^{181}Ta

M.S. MORENO, J. DESIMONI, F.G. REQUEJO, M. RENTERÍA, A.G. BIBILONI
Departamento de Física, Universidad Nacional de La Plata, CC No. 67, 1900 La Plata, Argentina

and

K. FREITAG
Institut für Strahlen und Kernphysik der Universität Bonn, Nussallée 14–16, 5300 Bonn, Germany

Received 12 December 1990

In connection with a general study of the evolution of tin–oxygen thin films, we report here on the hyperfine interactions of ^{181}Ta substitutionally replacing tin in the isolated phases SnO and SnO_2. For this purpose, pure SnO pressed powder and a thin SnO_2 film were implanted with ^{181}Hf. In both cases, unique quadrupole frequencies were found after thermal annealing treatments. The results indicate that the following hyperfine parameters: ν_Q = 740.6(2.1) MHz, η = 0.07(2) and ν_Q = 971.5(1.9) MHz, η = 0.72(1) characterize ^{181}Ta in SnO and SnO_2, respectively.

1. Introduction

The family of semiconductor thin films of SnO_2, In_2O_3, ITO (In_2O_3:Sn), CdO, etc. have been extensively used whenever an optically selective transparent coating is required. The case of tin dioxide is interesting due to its enormous practical potentiality, which latest application is in gas sensing devices. However, this wide spectrum of uses has no correspondence with the present knowledge of basic properties such as its quality of growing in different crystalline modifications (cubic, orthorhombic) [1]. Another unclear aspect is the transit of SnO to SnO_2 under various conditions. This situation originates in the production of intermediate phases and the impossibility of isolating them. In this respect, the study of ordinary specimens of these oxides, tetragonal SnO and SnO_2, is needed.

Hyperfine techniques like Mössbauer Spectroscopy (MS and CEMS) and Perturbed Angular Correlation (PAC), capable of distinguishing the presence of simultaneous phases and following the evolution of parameters related to the local order, can be suitable for this purpose.

Recently, we began the study of the evolution of thin films prepared by thermal evaporation of metallic tin in low oxygen pressure by CEMS and PAC. The resulting films were admixtures of different Sn–O disordered compounds with two different oxidation states for Sn. ^{119}Sn and implanted ^{181}Hf ions were employed in CEMS and

PAC measurements, respectively. As a result of increasing temperature annealing treatment, the crystallization of SnO, the formation of Sn_3O_4, and the achievement of the higher oxide SnO_2 were established. Tentative assignments for the hyperfine parameters of ^{181}Ta substitutionally replacing tin in SnO and SnO_2 [2], as well as those corresponding to the Sn^{2+} oxidation state in Sn_3O_4, were made [3]. Concerning the PAC measurements, the fact that SnO decomposed at medium temperatures, the impossibility of obtaining isolated Sn_3O_4, and the possible influence of the impurities (PAC probes) in the local crystallization made a definite assignment difficult.

2. Experimental

Tin monoxide powder, from Baker, 99.999% pure, was pressed into the form of a pill with a diameter of 8 mm and a thickness of 1 mm. X-ray spectrograms showed only the characteristic reflexions corresponding to the tetragonal phase reported in ref. [4].

The tin dioxide sample was prepared as follows: a thin film of about 300 nm, prepared by thermal evaporation of metallic Sn (99.999% pure) on a quartz substrate kept at room temperature in a 10^{-3} Torr oxygen atmosphere, was subsequently heated in air to 673, 1043 and 1373 K. Each treatment lasted 2 h. The CEMS spectrum taken on this sample showed the sole presence of tetragonal tin dioxide.

^{181}Hf ions with energies of 140–145 keV were implanted in both samples using the ion accelerator of the I.S.K.P. The total doses were 1.5 and 1.4×10^{13} ions/cm^2 for SnO and SnO_2, respectively.

A three-detector CsF fast-slow coincidence system in a coplanar 90° arrangement with a time resolution of 0.8 ns was used for data acquisition. Four coincidence spectra of all possible start-stop combinations of the three detectors were recorded simultaneously at each detector position in a multichannel analyzer. The $N(\theta, t)$ spectra, corrected for accidental counts, were combined in the following form to obtain the asymmetry ratio $R(t)$:

$$R(t) = \frac{2}{3}\left[\left(\frac{C_{13}(180,t)C_{24}(180,t)}{C_{14}(90,t)C_{23}(90,t)}\right)^{1/2} - 1\right] \cong A_2^{\exp} G_2(t), \tag{1}$$

where $A_2^{\exp}$ is the measured anisotropy of the γ–γ cascade and $G_2(t)$ is the perturbation factor. The EFG is described by two parameters: the quadrupole interaction frequency $\nu_Q = eQV_{zz}/h$ and the asymmetry parameter $\eta = (V_{xx} - V_{yy}/V_{zz}$. Using a nonlinear least-squares fit program that takes into account the finite time resolution of the equipment, the function

$$A_2 G_2(t) = \sum_i f_i \sum_{n=0}^{3} s_{2n,i}(\eta) \cos(\omega_{n,i}\, t) \mathrm{e}^{-\delta_i \omega_{n,i}} \tag{2}$$

derived from ref. [5] for a static quadrupole interaction in polycrystalline samples, was fitted to the experimental data. f_i are the relative fractions of nuclei that experience

a given perturbation. The ω_n frequencies are related by $\omega_n = g_n(\eta)\nu_Q$ to the quadrupole coupling constant $\nu_Q = eQV_{zz}/h$. The g_n and s_n coefficients are known functions [6] of the asymmetry parameter η. The exponential functions account for a Lorentzian frequency distribution of relative width δ around ω_n.

3. Results and discussion

Figure 1 shows the PAC spectra taken at room temperature on the SnO sample after annealings in argon, all lasting 1 hour, at 523, 573, 673 and 773 K, respectively.

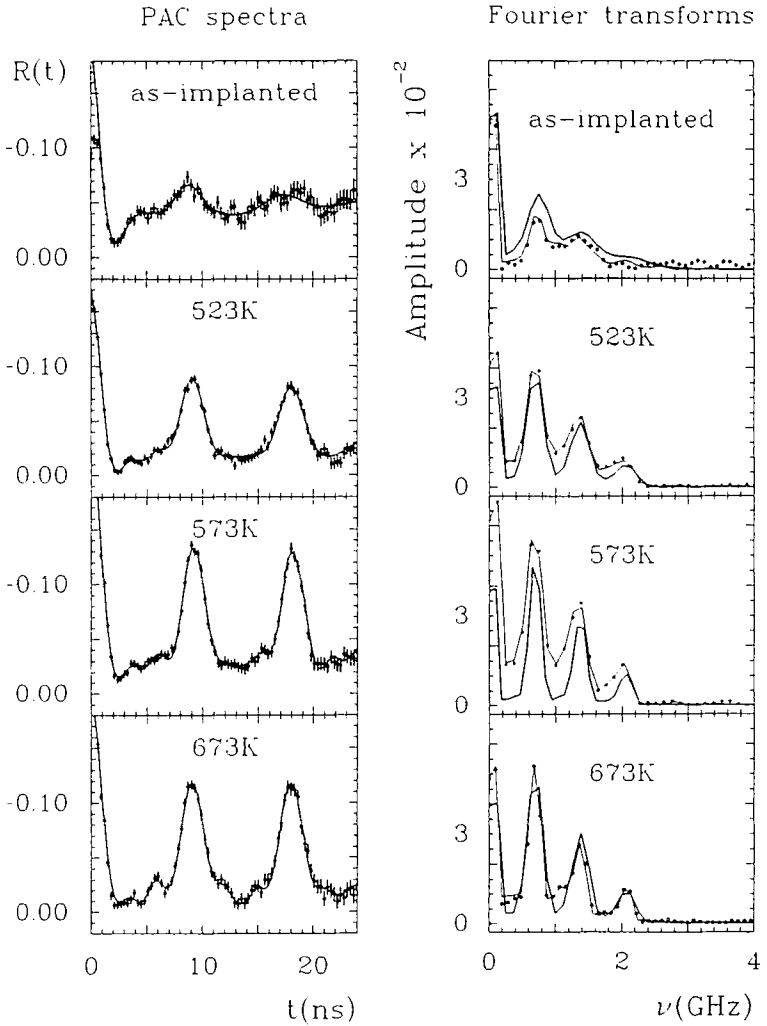

Fig. 1. PAC and Fourier spectra of the SnO powder samples, taken at room temperature, labeled according to the successive 1 h annealing treatment in Ar. The full lines are fits to the data. In the Fourier spectra, the bold full line is the transform of the result of the fit with only one quadrupole frequency.

The figure includes the spectrum taken immediately after the implantation. A drastic change in the hyperfine pattern is apparent, achieving, after the annealing at 573 K, an almost monochromatic aspect (this behaviour is evidenced in the Fourier spectra also included in fig. 1). Two and sometimes three hyperfine interactions were used in the fitting process to take into acount all their features. However, with regard to the characterization of the sample, the relevant aspects of the spectra are well fited with just one hyperfine interaction, as is shown on the right-hand side of the figure. In effect, the Fourier transform (bold full line) of the fit with only one quadrupole frequency is shown. This well-defined hyperfine interaction, characterized by ν_Q = 740.6(2.1) MHz and η = 0.07(2), was established after annealing at 523 K and remained stable up to 773 K, where it is replaced by a widely distributed interaction.

This well-defined interaction characterizing ^{181}Ta substitutionally replacing Sn in SnO coincides with that observed in ref. [2] during a study of the evolution of a thermally evaporated Sn–O thin film, and was tentatively attributed to the SnO crystalline. In effect, in that experiment – after annealing at 573 K in argon – the presence of an electric quadrupole frequency, characterized by ν_Q = 745 MHz and η = 0.1 with relative intensity f = 12%, was found superimposed on a broad distribution centered at ν_Q = 1044 MHz. This was assigned to ^{181}Ta in SnO since CEMS measurements on a similarly treated film revealed that after annealing at 573 K, the Sn^{2+} oxidation state showed the parameters that characterize Sn in SnO. The present results confirm that assignment. Furthermore, in agreement with the results of ref. [7], they reveal that this oxide is stable up to about 673 K.

Now, according to its crystalline structure, this oxide exhibits a unique crystallographic site for tin. In effect, the crystal structure of SnO is tetragonal [8]. The tin 2+ ions are in the apex of a square pyramid. This disposition yields a plate-like crystallographic morphology for SnO and gives an open structure where the substitution of Sn by Hf is favoured. Point charge model calculation, performed using the lattice parameters reported in ref. [8], results in an asymmetry parameter η = 0.0. Our results are in good agreement with these facts.

Figure 2 shows PAC spectra taken at room temperature on the SnO_2 crystalline film after ion implantation and annealing treatments at 673 and 1073 K. The annealings, both lasting 1 h, were performed in air. Fourier spectra are also included, as well as the results of the fitting process. Again, a well-defined hyperfine interaction is noticeable in the whole series. However, an improvement of the pattern is seen as the annealing temperature increases, achieving, after annealing at 1073 K, its best feature. The least-squares fits revealed that the major fraction of probes, f = 90%, correspond to probes experiencing a hyperfine interaction characterized by ν_Q = 971.5(1.9) MHz and η = 0.72(1), which should be attributed to ^{181}Ta substitutionally replacing tin in SnO_2. Since this interaction is present from the very beginning, the only change evidenced is due to radiation damage recovery.

The present results agree with those obtained in ref. [2] for the final stage of the evolution of an Sn–O film, and show that the presence of a few ppm of the impurity ^{181}Hf did not affect the local crystallization of the film in the form of SnO_2.

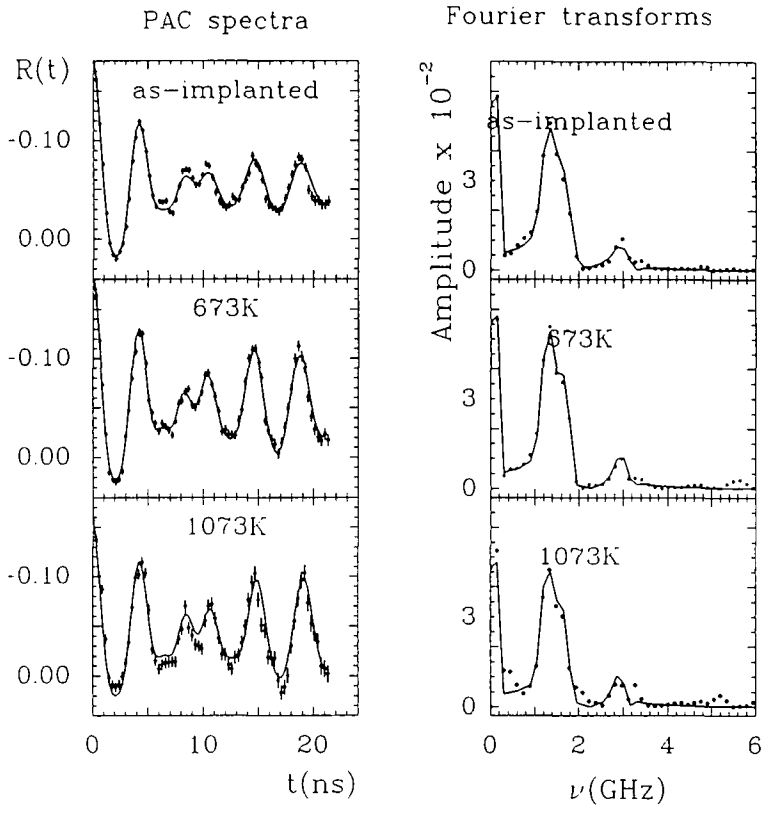

Fig. 2. PAC and Fourier spectra of the SnO_2 thin film sample, taken at room temperature, labeled according to the successive 2 h annealing treatment in air. The full lines are fits to the data.

In contrast to the case of SnO, in the stannic oxide Sn^{4+} are placed in a distorted octahedra, giving a crystalline structure of rutile type where oxygen ions are stacked in an approximated HCP array [9].

Point charge calculations have been done using the crystallographic data of ref. [9]. The predicted asymmetry parameter is 0.2. This value does not fit our results. The fact that the ionic radius of the probe (^{181}Hf) is larger than that of Sn (0.81 and 0.71 Å, respectively), as well as the different electronic structures, makes it difficult to predict how the local structure changes. Small changes in the local configuration, i.e. an elongation in the octahedra axis formed by the oxygen near-neighbours of just 2.2%, give rise to an η of 0.7. Unfortunately, theoretical calculations for this type of lattice-impurity relaxation do not exist in the literature.

Other interesting information can be obtained from comparison of PAC results with point charge model calculations.

According to Bolse et al. [10], the antishielding factor β, defined as $\beta = \nu_Q^{exp}/\nu_Q^{theor}$, where ν_Q^{exp} and ν_Q^{theor} are the experimental and calculated quadrupole

coupling constants, respectively, is mostly determined by the nearest-neighbour (NN) oxygen coordination, increasing with the number of NN oxygen ions. The authors reached this conclusion from the available evidence on ^{111}In implanted oxides. Our results, $\beta_{SnO} = 71.9(1.5)$ and $\beta_{SnO_2} = 99.5(2.1)$, are in agreement with these statements; the antishielding factor for ^{181}Ta in stannic oxide (sixfold coordination) is larger than the corresponding one in stannous oxide (fourfold coordination).

Acknowledgements

The authors acknowledge Lic. H. Viturro, Centro de Investigaciones y Desarrollo de Procesos Catalíticos (CINDECA, Argentina) for X-ray characterization. This work was partially supported by the Consejo Nacional de Investigaciones Científicas y Técnicas (CONICET) and the Kernforschungzentrum Karlsruhe GmbH, Germany.

References

[1] S.K. Peneva, R.K. Rudarska, D.D. Nihtianova and I. Avramov, Thin Solid Films 112(1984)247; K. Suito, N. Kawai and Y. Masuda, Mat. Res. Bull. 10(1975)677.
[2] M.S. Moreno, J. Desimoni, A.G. Bibiloni, M. Rentería and C.P. Massolo, Phys. Rev. B (in press).
[3] M.S. Moreno, J. Desimoni, R.C. Mercader and A.G. Bibiloni, in: *Proc. II Latin American Conf. on the Applications of the Mössbauer Effect*, Havana (1990), Hyp. Int. (1991), to be published.
[4] Powder Diffraction Files, Card 6-0395.
[5] H. Frauenfelder and R.M. Steffen, in: *Alpha-, Beta-, and Gamma-ray Spectroscopy*, ed. K. Siegbahn (North-Holland, Amsterdam, 1966), p. 1183.
[6] L.A. Mendoza Zélis, A.G. Bibiloni, M.C. Caracoche, A.R. López-García, J.A. Martínez, R.C. Mercader and A.F. Pasquevich, Hyp. Int. 3(1977)315.
[7] H. Spandau and E.J. Kohlmeyer, Z. Metallkunde 40(1949)374.
[8] J. Pannetier and G. Denes, Acta Cryst. B36(1980)2763.
[9] R.M. Hazen and L.W. Finger, J. Phys. Chem. Solids 42(1981)143.
[10] W. Bolse, A. Bartos, J. Kesten, M. Uhrmacher and K.P. Lieb, *XIII Zakopane School on Physics*,, Kracow (1988).